

Research Journal of Applied Sciences Engineering and Technology 4(10): 1268-1276, 2012

ISSN: 2040-7467

© Maxwell Scientific Organization, 2012

Submitted: November 28, 2011

Accepted: January 04, 2012

Published: May 15, 2012

Numerical Optimization of Cylinder Flow Structure of CO₂ Laser

¹Jiang Fan and ²He Hua

¹School of Mechanical and Electric Engineering, Guangzhou University, Guangzhou, 510006, China

²Department of Mechanical and Electric Engineering, Bengbu College, Anhui 233030, China

Abstract: The cylinder flows structure is important part in the transverse-flow CO₂ laser, which affects the internal gas flow, and influences the flow kinetic energy loss. To study structural optimization to reduce the flow kinetic energy loss is a key concern of designers. In this study, the dynamic mesh model is used to simulate the rotation of cross-flow fan, the calculation process shows that it is easy to understand how to set parameter and treat mesh. Through optimization analysis on six structure parameters of the cylinder flow, we obtain the results that some of the parameters significantly influence the mixture gas velocity distribution in the discharge domain, but some other parameters of the flow field less affected velocity distribution of the discharge domain. The variation trends of the velocity distribution is also inconsistent which impacted by variation of each parameter. Through comprehensive analysis, the results of the optimization are: $\alpha_1 = 14$; $\alpha_2 = 67.9$; $\alpha_3 = 73.1$; $\alpha_4 = 9.5$; $\alpha_5 = 65.6$; $\alpha_6 = 41.7$. By validation calculations for the optimized structure of cylinder flow, we obtain the results that the flow state of discharge domain in the optimized structure is better than that of the previous structure.

Key words: CO₂ laser, cylinder flow structure, dynamics mesh, numerical optimization

INTRODUCTION

The transverse-flow CO₂ laser is one of the most important high-power lasers; its fluid-dynamical circuit designed in cylindrical geometry is a very compact and simple device; it's cheaper, and has low dimensions and operating costs (Gutu *et al.*, 2003; Martín *et al.*, 2005; Li and Huang, 2005). Cylinder flow structure is a flow structure of the transverse-flow CO₂ lasers; it is attended in view of it's very compact. Although it has shorter air compressor and diffuser, the kinetic energy loss is greater (Li and Huang, 2005). The structure affects the internal gas flow which in turns influences the flow kinetic energy loss. It is necessary to study structural optimization to reduce the flow kinetic energy loss. During the past, there were some researches on flow field and temperature field of transverse-flow CO₂ lasers; the relationship between flow field and structure is discussed (Han, 2005; Li, 2009). However, these references mainly focus on the raceway flow structure of the transverse-flow lasers; less data has been obtained on optimization analysis of the structure of cylinder flow structure in CO₂ lasers.

In the traditional method, the relationship between structure and flow field is obtained by experiment; so the optimization analysis is a difficult task due to high cost and relatively long verification period. With the development of numerical simulation technology,

Computational Fluid Dynamics (CFD) techniques can offer a cost-effect solution for flow structure optimization. The temperature model of transverse-flow CO₂ laser with race-way flow structure is built in ANSYS, and its working statements in different conditions are simulated, the temperature distribution results in the way of flowing gas CO₂ laser are obtained (Han, 2005). The flow field inside of fast-axial-flow CO₂ lasers was analyzed by the software FLUENT, also the key factors were explained which has influence on the stability of glow discharge (Li, 2009). Cross-fan is a key part in the transverse-flow CO₂ lasers with cylinder flow structure, and the fan is high-speed rotating in work, so the internal flow simulation is dynamic simulation. Dang and Bushnell (2009) review and compare to unsteady calculations using sliding mesh method, these unsteady will predict the detailed flow field in a cross-flow fan (Dang and Bushnell, 2009). Gebrehiwot *et al.* (2010) use the sliding mesh model to simulate the flow configuration and performance of a cross-flow fan, and demonstrated that 2D CFD model can predict fan performance up to is unavailable (Gebrehiwot *et al.*, 2010). Moreover, little information has been done on analyzing the flow field and optimizing the cylinder in which the transverse flow of CO₂ laser runs. In previous researches, the flow field of the rotating blade with cross-flow fan was simulated by the sliding mesh. But the dynamics mesh which is more realistic hasn't been used to simulate the blade rotation.

Corresponding Author: Jiang Fan, School of Mechanical and Electric Engineering, Guangzhou University, Guangzhou, 510006, China

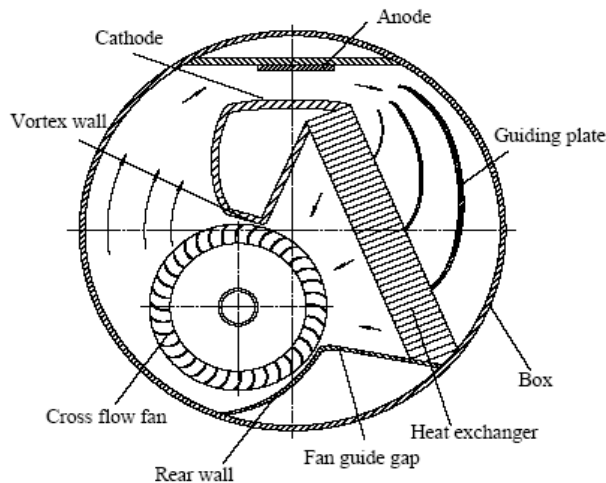


Fig. 1: Structure of cylinder flow CO₂ laser

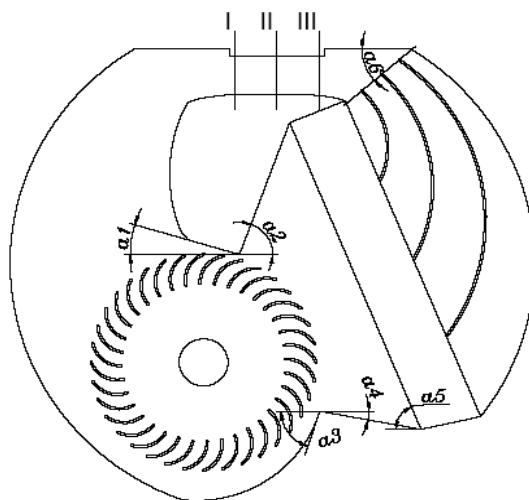


Fig. 2: Simplified model

In this study, the dynamics mesh model is used to simulate the rotating blade of transverse-flow CO₂ laser with cylinder flow structure. It is easier to be understood than sliding mesh mentioned in references (Dang and Bushnell, 2009; Gebrehiwot *et al.*, 2010). The cylinder flow structure is optimized; it provides data to the cylindrical flow structure design. It explains how the specific set of design parameters impacts on a given performance and efficiency which not mentioned in the references.

COMPUTATIONAL MODELS

In Fig. 1, the cylinder flow structure consists of cross-flow fan, air-gap plate, heat exchangers, guiding plate, discharge area, tank box and other components.

Figure 2 is the simplified model. According to previous studies (Gebrehiwot *et al.*, 2010; Toffolo, 2005), the rear wall and vortex wall play key role on cross-fan performance. However, the rear wall and vortex wall are affected by size parameters; they are α_1 , α_2 , α_3 and α_4 , and they also could influence inflow arc, outflow arc, and the velocity distribution of discharge domain. From our experiment, the parameters α_5 and α_6 could influence the gas flow field inside of CO₂ laser; so these parameters are acted as the optimization variables in the next step calculation.

The internal flow structures of cylinder flow are optimized by calculating the flow inside of cylinder; the CFD software FLUENT 6.3.26 is used (Jiang *et al.*, 2008a, b; Jiang *et al.*, 2009; Jiang *et al.*, 2010a, b, c, d). The transient, 2D, viscous, compressible unsteady

Reynolds-averaged Navier-Stokes equations were solved. The RNG k-ε model was adopted to describe the effects of turbulence. The pressure term is discretized by standard scheme; the density, the momentum, and the turbulent kinetic energy terms are discretized by first order upwind scheme; the pressure-velocity coupling equations are solved by the SIMPLE (semi-implicit method for pressure-linked equations) algorithm. Because of the highly transient flow in the blade channels, the calculation was performed unsteady.

The blade rotation of cross-fan is unsteady; most researcher captured this unsteady interaction by the unsteady “sliding mesh” CFD method; but this technique will divide the computational domain into two types of zones; thus it leads to much too trouble in setting the grids and computing parameters. Dynamic mesh is easier to understand; and it needn't divide difference zone; so the dynamic mesh technology is used in this calculation; the equation is as following:

$$\frac{d}{dt} \int_{V_s} \rho \phi dV + \int_{L_s} \rho \phi (u - u_g) n dS = \int_{L_s} \Gamma \nabla \phi n dS + \int_{V_s} q \phi dV \quad (1)$$

Here, φ is general variable; V_s control volume; L_s boundary of the control volume; u average velocity; u_g moving velocity of dynamics mesh; n normal unit vector on surface outwards.

The domains of heat exchanger are simulated by porous media model. This model has an additional of a momentum source term. Outside the standard fluid flow equations, the term covers the simple homogeneous porous media. The term is written as:

$$\Delta p = \left(\frac{\mu}{\alpha} v + \frac{C_2}{2} \rho v^2 \right) \quad (2)$$

Here, α is the permeability, C₂ the inertial resistance factor; α and C₂ are obtained by experiment; the computation method is described as following:

$$\alpha = \frac{\mu}{\frac{p_1^2 - p_2^2}{2Lp_1u_1} - \frac{p_1u_1}{2L(p_1u_1 - p_2u_2)} \left(\frac{p_1}{u_1} - \frac{p_2}{u_2} - \frac{p_{01}^2}{p_1u_1} + \frac{p_{02}^2}{p_2u_2} \right)} \quad (3)$$

$$C_2 = \frac{RT}{2L(p_1u_1 - p_2u_2)} \left(\frac{p_1}{u_1} - \frac{p_2}{u_2} - \frac{p_{01}^2}{p_1u_1} + \frac{p_{01}^2}{p_2u_2} \right) \quad (4)$$

In above equations, p₁ and u₁ are the pressure and velocity respectively about the first condition in front of porous region; p₀₁ the pressure of the first condition behind of porous region; p₂ and u₂ are pressure and velocity of the second condition in front of porous region respectively; p₀₂ the pressure of the second condition

Table 1: Geometric parameters of the computation domain

Parameter	Value
C _{cylinder}	300 mm
R _{Outer-circle-blade}	127.88 mm
R _{Inner-circle-blade}	98.36 mm
B _{blade}	31.27 mm
S _{haft}	28 mm
D _{ischarge}	108.24 mm
E _{xchanger}	68.84 mm
T _{total}	537.34 mm
D _{ischarge}	45 mm
α1	16.0
α2	69.9
α3	72.0
α4	10.5
α5	67.6
α6	40.7

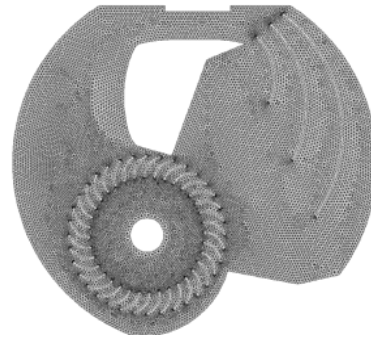


Fig. 3: Initial grid model

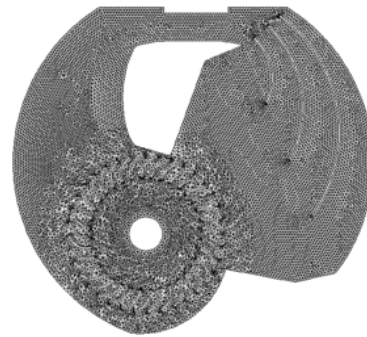


Fig. 4: Grid model after running 0.2 s

behind of porous region; R the thermodynamic constants of 8.314; T temperature; L length of porous region. The porosity of heat exchange is 0.8107. Obtained by experiment, α is 1.324e7, C₂ 0.0024.

TRANSIENT ANALYSIS INSIDE OF CYLINDER FLOW

Figure 2 shows the calculation domain; Table 1 the geometric parameters. The parameters α1, α2, α3, α4, α5 and α6 are to be optimized. The calculation domain is meshed by triangle grids. In the dynamics mesh model, the initial cells number is 27194, the nodes number 14456. Figure 3 shows grid model; Fig. 4 is the grid after

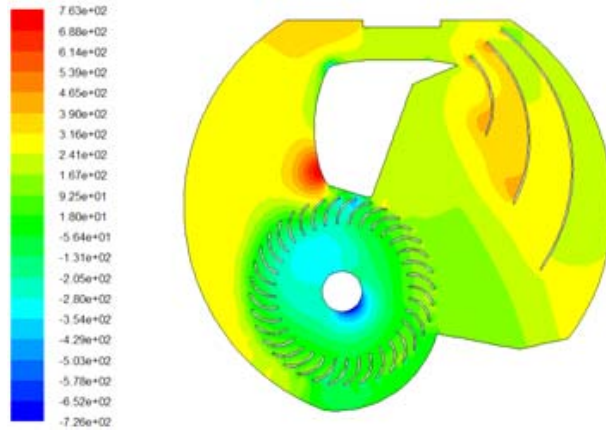


Fig. 5: Pressure contour at 0.2 s

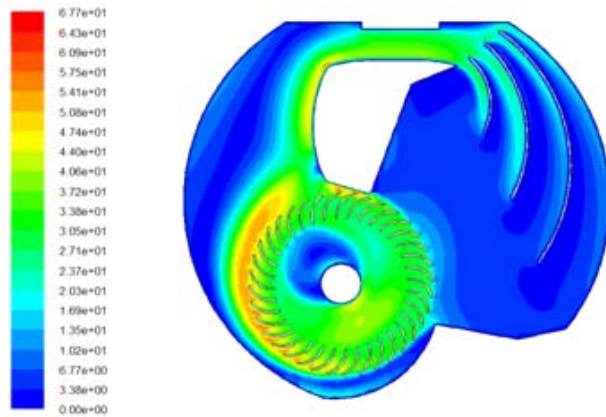


Fig. 6: Velocity contour at 0.2 s

turning 0.2s. The blades angular velocity is 2800 rpm; the time step of the unsteady calculation, Δt , $2e-5$ s.

The fluid gas was mixture, ideal; its viscosity is $2.313e-5$ kg/m/s; the thermal conductivity 0.0925W/K; C_p 1.943 kJ/(kg-k); molecular weight 12.28 kg/mol.

After being set the given fluid material properties, the blade rotational velocity, and the porous media parameters, through the numerical calculation (calculated time is 0.2s), many flow field results (including pressure, velocity, streamline, turbulence, etc.) are obtained. Because pressure and velocity are the key factor of the discharge performance of CO₂ lasers, it needs the pressure and velocity contours. They are shown in Fig. 5-6.

Figure 5 shows the pressure field of calculation domain. The pressure field results could help us to analyze the flow efficiency of CO₂ laser. At this time, there is the maximum pressure at the top of cross fan outlet, the minimum pressure under of shaft, and more balanced pressure in discharge domain.

The pressure loss information could be obtained from this figure; it affects the flow efficiency. Its values at two

ends of discharge domain are relatively large due to here mixture gas turn around sharply. Especially at the back end of discharge, the pressure variation is large. The pressure at intake is little, and at outlet is great. This makes the mixed gas flow into cross-fan from the intake, and flow out cross-fan from the outlet.

Figure 6 shows the condition that the mixed gas flows in the calculation domain. The maximum velocity is at the outlet of cross-fan, and the minimum velocity is in the heat exchanger and at the front of discharge domain.

The variation of pressure and velocity in discharge domain could impact discharge performance of CO₂ laser. The variation curve of pressure and velocity are obtained at I-III lines (Fig. 2, the line I-III are lines respectively in the inlet, the center, the outlet of discharge domain) from numerical calculation, and shown in Fig. 7-10.

Figure 7 shows the pressure variation in the different location; the pressure distribution of different lines are large different; the pressure variation is greater at the entrance. But the pressure of the central line is similar. Figure 8 shows the velocity variation in the different

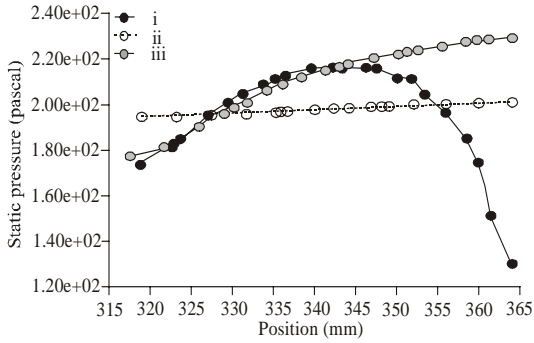


Fig. 7: Pressure distribution in different location

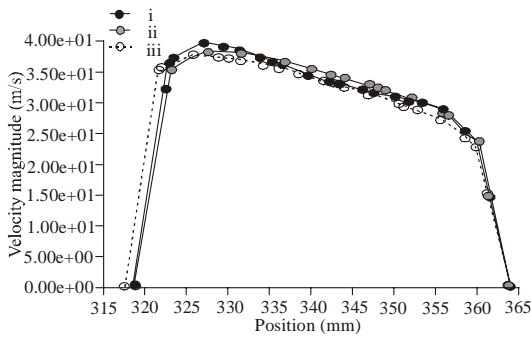


Fig. 8: Velocity distribution in different location

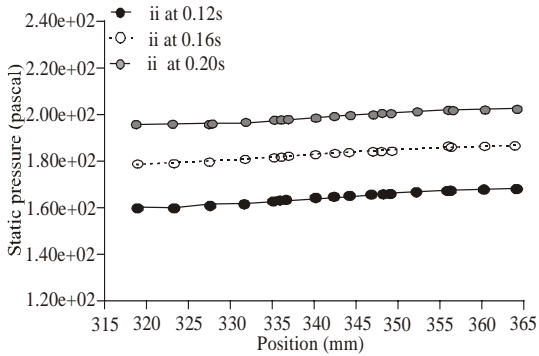


Fig. 9: Pressure distribution at different time

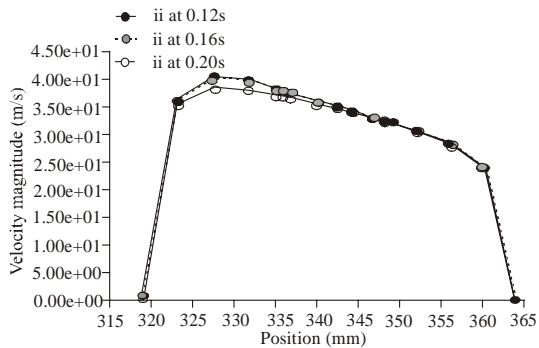


Fig. 10: Velocity distribution at different time

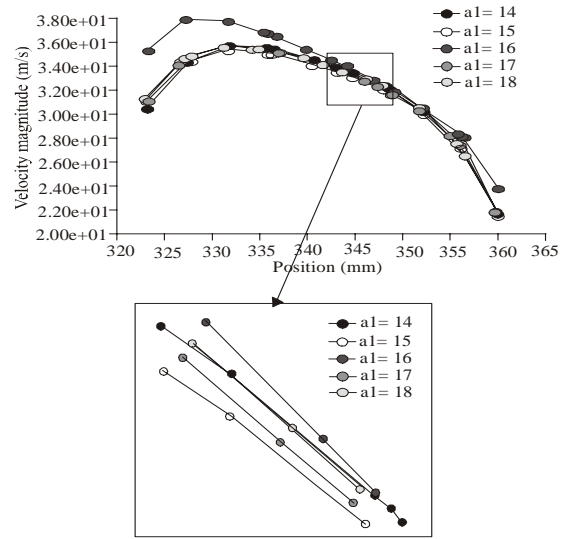


Fig. 11: Velocity comparison of different $\alpha 1$

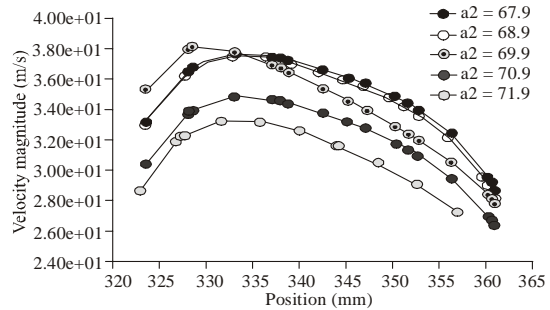


Fig. 12: Velocity variation of different $\alpha 2$

location; the velocity distribution of different lines is similar. The velocity at bottom of discharge domain is greater than that in top of discharge domain.

Figure 9 shows the pressure distribution on line II at different time; it has obvious difference. Figure 10 shows the velocity variation on line II at different time, it has similar shape. From these figures, the velocity is relatively stable with little impacted by location and operation time; but the pressure varies at different time at different location. Therefore, acted as the evaluation index in the structural evaluation next steps, the velocity is reasonable.

STRUCTURE OPTIMIZATION OF CYLINDER FLOW

Influence of size $\alpha 1$: Size $\alpha 1$ is angle between horizontal surface and back surface of vortex wall; it could affect the outflow arc. To investigate on the influence of size $\alpha 1$ of the cylinder flow to the velocity of mixture gas, five different calculation were analyzed with different $\alpha 1$ and the grid parameters, shown in Table 2. The velocity distributions on the center line of discharge domain of different models are shown in Fig. 11.

Table 2: Model parameters of different α_1

No.	α_1	Cells	Nodes
M1	14	27098	14407
M2	15	27106	14412
M3	16	27194	14456
M4	17	27162	14440
M5	18	27166	14442

Table 3: Model parameters of different α_2

No.	α_2	Cells	Nodes
M6	67.9	27248	14482
M7	68.9	27218	14468
M8	69.9	27194	14456
M9	70.9	27200	14459
M10	71.9	34230	18092

Table 4: Model parameters of different α_3

No.	α_3	Cells	Nodes
M11	72.1	27164	14441
M12	73.1	27124	14421
M13	74.1	27194	14456
M14	75.1	27230	14474
M15	76.1	27264	14494

Figure 11 shows the velocity difference neared the lower wall of the discharge domain. It is relatively large in different models, and is little near the upper wall. Most velocity distribution curves almost coincide; it indicates that parameter α_1 is little effect on the gas velocity of the discharge domain. As $\alpha_1 = 16$, the velocity distribution significantly greater than the others; but there is great difference between its two ends. Based on comparing the velocity value and distribution characteristic, $\alpha_1 = 14$ is the optimum value.

Influence of size α_2 : Size α_2 is angle between horizontal surface and the front surface of vortex wall; it influences the inflow arc. In order to understand the relationship of size α_2 and the flow field in CO₂ laser, five different models were analyzed with different α_2 , and the grid parameters shows in Table 3. The velocity distributions on the center line of discharge domain of different models are shown in Fig. 12.

From Fig. 12, the size α_2 has a great influence on mixture gas velocity. As α_2 increases, the gas velocity of discharge domain increases, too. The curve of $\alpha_2 = 67.9$ is very similar with that of $\alpha_2 = 68.9$; the former is slightly higher than the latter; and the others have obvious difference. The velocity distribution of $\alpha_2 = 67.9$ has more uniform and smooth, so it is recommended values.

Influence of size α_3 : Size α_3 is angle between horizontal surface and the surface of rear wall, it influence the outflow arc. In order to discuss the relationship of size α_3 and the flow field in CO₂ laser, five different models were analyzed with different α_3 and the grid parameters, which

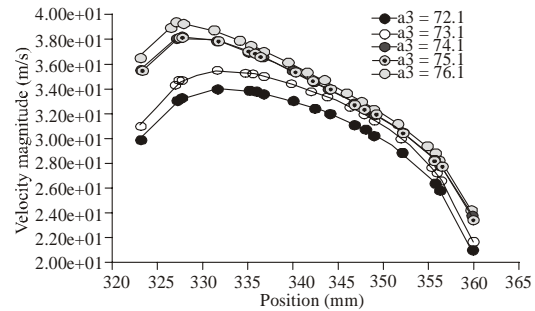


Fig. 13: Velocity curve of different α_3

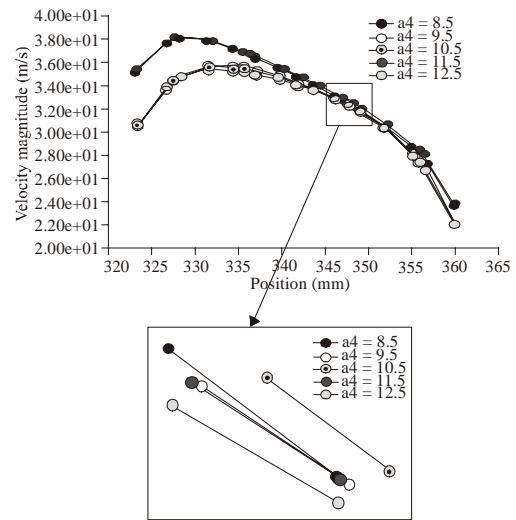


Fig. 14: Velocity curves of different α_4

line of discharge domain of different models are shown in Fig. 13.

From Fig. 13, as the size α_3 increases, the flow shown in Table 4. The velocity distributions on the center velocity of discharge domain increases. The velocity curve $\alpha_3 = 76.1$ is higher than the others; it can be seen that there are greater velocity, but it is not uniform, which velocity on lower is much greater than on upper. Comprehensive comparison of the velocity curve in Fig. 13, the $\alpha_3 = 73.1$ is suitable.

Influence of size α_4 : Size α_4 is angle between the horizontal surface and the leading surface of rear wall; it influences the inflow arc. In order to analyze the influence of size α_3 to the flow field of discharge domain, five different models were analyzed with different α_4 and the grid parameters, which shown in Table 5. The velocity distributions on the center line of discharge domain of different models are shown in Fig. 14.

Figure 14 indicates that the velocity curves $\alpha_4 = 8.5$ and $\alpha_4 = 10.5$ are much closed to each other, and the other three curves are very close to each other. The velocity

Table 5: Model parameters of different α_4

No.	α_4	Cells	Nodes
M16	8.5	27106	14411
M17	9.5	27158	14433
M18	10.5	27194	14456
M19	11.5	27172	14445
M20	12.5	27202	14460

Table 6: Model parameters of different α_5

No.	α_5	Cells	Nodes
M21	65.6	27266	14486
M22	66.6	27166	14438
M23	67.6	27194	14456
M24	68.6	34096	18027
M25	69.6	27098	14413

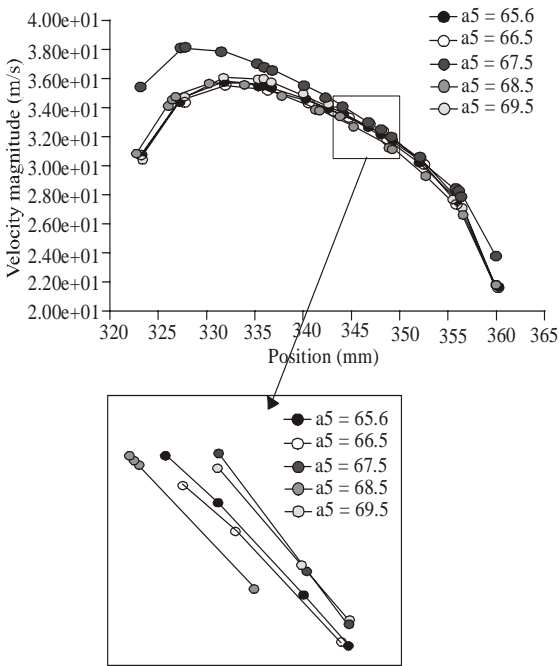


Fig. 15: Velocity curve of different α_5

curves $\alpha_4 = 8.5$ and $\alpha_4 = 10.5$ have great velocity difference at two ends; however, the velocity curves $\alpha_4 = 9.5$, $\alpha_4 = 11.5$ and $\alpha_4 = 12.5$ has relatively uniform velocity; the curves $\alpha_5 = 9.5$ is slightly higher. Comprehensive comparison of the velocity curve in Fig. 14, the $\alpha_5 = 9.5$ is ideal.

Influence of size α_5 : Size α_5 is the angle between section of the heat exchanger and the horizontal, which indirectly reflects the impact of impeding the heat exchanger on the flow field. In order to probe the relationship of size α_5 and the flow field in CO₂ laser, five different models were analyzed with different α_5 and the grid parameters, as shown in Table 6. The velocity distributions on the center line of discharge domain of different models are shown in Fig. 15.

Table 7: Model parameters of different α_6

No.	α_6	Cells	Nodes
M26	38.7	27174	14443
M27	39.7	27156	14435
M28	40.7	27194	14456
M29	41.7	27218	14468
M30	42.7	27162	14441

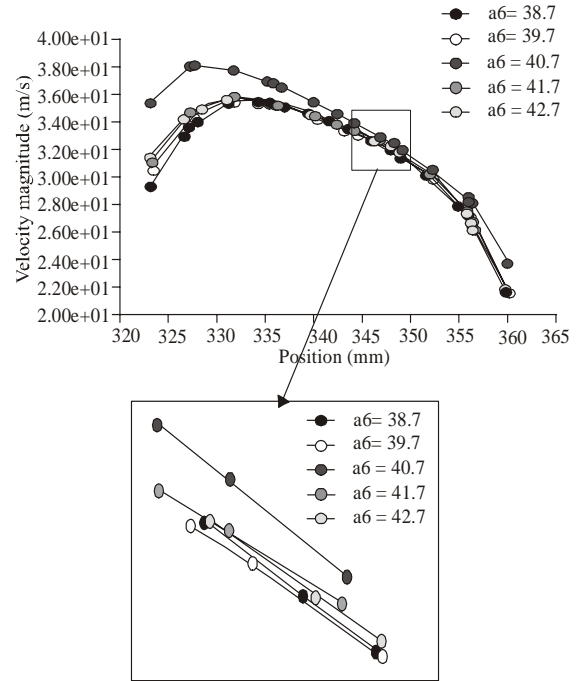


Fig. 16: Velocity curve of different α_6

From Fig. 15, with increasing size α_5 , the velocity distribution develops differently, the velocity curve $\alpha_5 = 65.6$, $\alpha_5 = 66.6$, $\alpha_5 = 68.6$, and $\alpha_5 = 69.6$ are very closed to each other, the curve $\alpha_5 = 67.6$ is obviously higher, which has greater velocity, but has great difference on two ends. Comprehensive comparison of the velocity curve in Fig. 15, the $\alpha_5 = 65.6$ is suitable.

Influence of size α_6 : Size α_6 is angle between horizontal surface and the line connects to guiding plate entrance; it influences the flow in the outlet of discharge domain. In order to obtain the relationship of size α_6 and the flow field in CO₂ laser, five different models were analyzed with different α_2 and the grid parameters, which shown in Table 7. The velocity distributions on the center line of discharge domain of different models are shown in Fig. 16.

Figure 16 shows that as the size α_6 increases, the flow velocity of discharge domain increases first and then decreases. The velocity curve $\alpha_6 = 40.7$ is higher than the others, indicates that there are greater velocity; but it is not uniform, whose velocity difference is much greater.

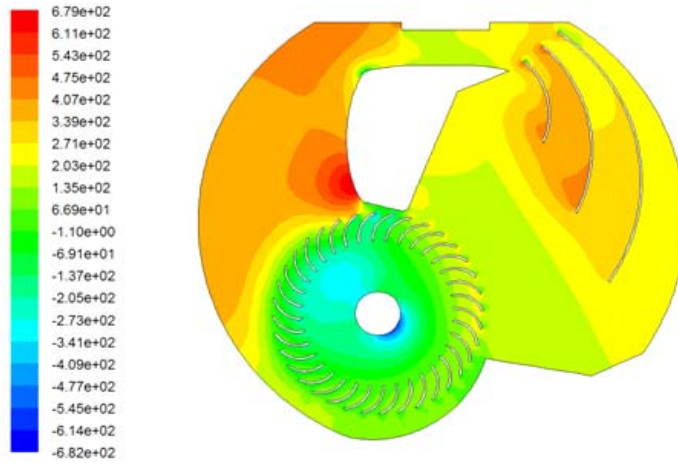


Fig. 17: Pressure contour of optimized model at 0.2 s

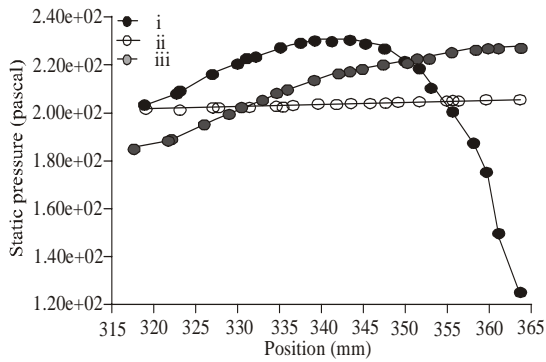


Fig. 18: Pressure distribution of optimized model in different location

Comprehensive comparison of the velocity curve in Fig. 16, the suitable α_6 is 41.7.

Based on the above analysis, the optimization parameters are: α_1 : 14; α_2 : 67.9; α_3 : 73.1; α_4 : 9.5; α_5 : 65.6; α_6 : 41.7.

Validation of optimized results: The structure of cylinder flow with the optimized parameters is numerical simulated; the grid model parameters are: 14494 nodes, 27282 cells, the results are shown in Fig. 17-20.

Figure 17 is pressure contour of the optimized model. Compared with Fig. 5, the pressure distribution has obvious difference. The maximum pressure decreases, and the pressure difference increases between two ends of discharge domain. Figure 18 shows the pressure distribution of I-III lines, the pressure difference between inlet and outlet is greater than that of old model, which is compared with Fig. 7.

Compared with Fig. 19 and 6, the velocity distribution is significantly more uniform. From Fig. 20, the velocity curve becomes more flat, and the velocity

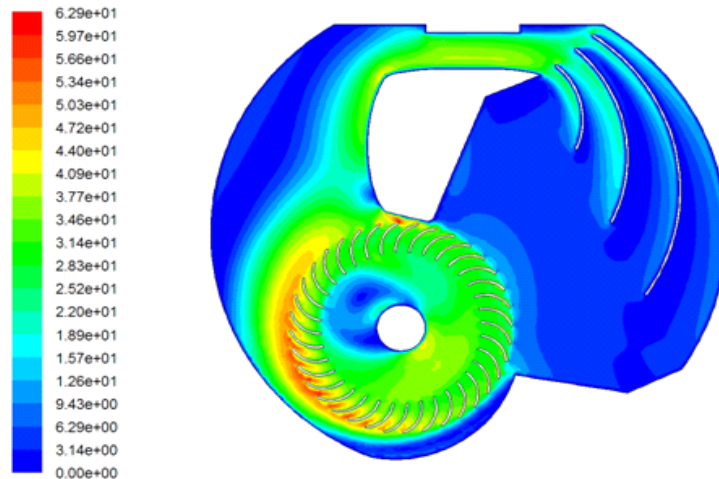


Fig. 19: Velocity contour of optimized model at 0.2 s

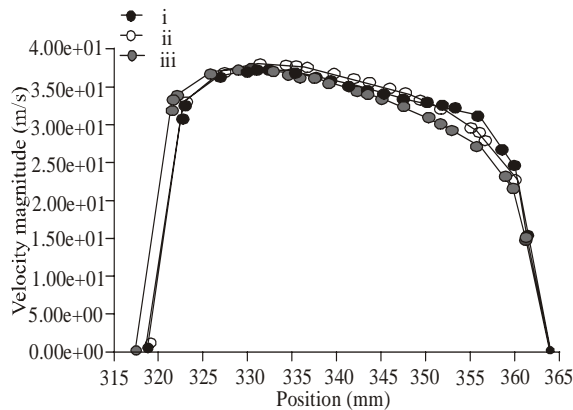


Fig. 20: Velocity distribution of optimized model in different location

on the three lines has little fluctuation, the velocity on the upper and lower of discharge domain are similar.

CONCLUSION

- Calculation practice shows that the calculation using the dynamic mesh model to simulate the rotation of cross-flow fan. The method is easier to understand, and the parameters are relatively easy to be set. For cylindrical flow of closed structure, just set rotating velocity of the cross-flow fan can be calculated.
- Through optimization analysis on the six structural parameters of the cylinder flow, the results show that, the influence of α_2 and α_3 is obvious to mixture gas velocity distribution of the discharge domain, but α_1 , α_4 , α_5 and α_6 has less affected to velocity distribution of the discharge domain. Impacted by the variation of each parameter, the variation trends of the velocity distribution is also inconsistent. As α_3 increases, the velocity distribution has trends to increase gradually. While the α_1 , α_2 , α_4 , α_5 and α_6 increase, the variation of velocity distribution is nonlinear. Through comprehensive comparison of the velocity absolute value and its distribution uniformity, the results of the optimization are: α_1 : 14; α_2 : 67.9; α_3 : 73.1; α_4 : 9.5; α_5 : 65.6; α_6 : 41.7.
- By validation calculations for the optimized structure of cylinder flow, the results show that the flow state of discharge domain in the optimized structure is better than that of the previous structure; the velocity is relatively great, and the velocity distribution is relatively uniform.

REFERENCES

Dang, T.Q. and P.R. Bushnell, 2009. Aerodynamics of cross-flow fans and their application to aircraft propulsion and flow control. *Prog. Aerosp. Sci.*, 45(1-3): 1-29.

Gebrehiwot, M.G., J.D. Baerdemaeker and M. Baelmans, 2010. Numerical and experimental study of a cross-flow fan for combine cleaning shoes. *Biosystems. Engine.*, 106(4): 448-457.

Gutu, I., C. Petre, I. Ivanov and I.N. Mihailescu, 2003. Optical resonator for high-power transverse flow CO₂ lasers. *Opt. Lasers Technol.*, 35(1): 105-113.

Han, Y.Z., 2005. Temperature Field Simulation and Parameter-Optimization of Way of flow Gas in the High-Power Transverse-Flow CO₂ Laser. Master Degree Dissertation, Wuhan University of Technology, Wuhan, China.

Jiang, F., W.P. Chen and Y.Y. Li, 2008a. Spatial structure injection molding analysis of suspended bio-carriers. *Mater. Sci. Forum*, 575-578: 385-388.

Jiang, F., W.P. Chen and Y.Y. Li, 2008b. Numerical evaluation of spatial structure of suspended bio-carriers. *J. South China Univ. Technol.*, 37(12): 75-79.

Jiang, F., X.C. Liu and C. Wang, 2009. Numerical simulation of soot particle flow indoor of automobile. *Proceedings of the 3rd International Conference on Mechanical Engineering and Mechanics*, 1: 1010-1015.

Jiang, F., J. Yu and Z.W. Liang, 2010a. New blood vessel robot design and outside flow field characteristic. *Appl. Mech. Mater.*, 29-32: 2490-2495.

Jiang, F., C.M. Huang and Z.W. Liang, 2010b. Numerical simulation of rotating-cage bio-reactor based on dynamic mesh coupled two-phase flow. *Lec. Notes Comp. Sci.*, 5938: 206-211.

Jiang, F., J. Yu and Z.M. Xiao, 2010c. Outside flow field characteristic of biological carriers. *Adv. Mater. Res.*, 113-114: 276-279.

Jiang, F., C.L. Zhang and Y.J. Wang, 2010d. Mechanical behavior analysis of CDIO production-blood vessel robot in curved blood vessel. *Lec. Notes Comp. Sci.*, 6377: 541-548.

Li, Q., 2009. Computational fluid dynamics modeling of discharge tube in Fast-axial-flow CO₂ Laser. PhD Thesis, Huazhong University of Science & Technology, Wuhan, China.

Li, S.M. and W.L. Huang, 2005. Principle and Design of Laser Devices. National Defence Industry Press, Beijing, China.

Martín, G.G., J.R. Ignacio and D. Violeta, 2005. An analytical approach to the design of electrodes in high-power, fast-transverse-flow lasers. *Opti. Laser Technol.*, 37(8): 615-622.

Toffolo, A., 2005. On the theoretical link between design parameters and performance in cross-flow fans: A numerical and experimental study. *Comp. Fluid.*, 34(1): 49-66.